

Generation of Broadband Snow Albedo  
Products from Resourcesat-2 AWIFS Data

— *a fully automated algorithm approach*

Geophysical Products Development Division  
Geophysical and Special Processing Group  
Satellite Data Acquisition & Products Services Area  
National Remote Sensing Centre (ISRO)  
Balanagar, Hyderabad.  
Nov. 2014

---



---

NATIONAL REMOTE SENSING CENTRE

---



---

## DOCUMENT CONTROL SHEET

1.	<b>Security classification</b>	Restricted			
2.	<b>Distribution</b>	Within ISRO/DOS			
3.	<b>Document (a) Issue:</b>	<b>01</b>	<b>(b) Revision:</b>	-	
4.	<b>Report Type</b>	Technical			
5.	<b>Report No</b>	NRSC-SDAPSA-G&SPG-NOV-2014			
6.	<b>Title</b>	Generation of broadband Snow Albedo Products from Resourcesat-2 AWIFS sensor data – a fully automated algorithm approach			
7.	<b>Collation</b>	<b>Pages</b> 17	<b>Figures</b> 8	<b>Tables</b> 2	<b>References</b> 10
8.	<b>Project</b>	Land Geophysical Products from IRS Missions			
9.	<b>Author(s)</b>	P.K. Saritha, V. Keerthi, S. Jayabharathi, S. Suresh and A. Senthil Kumar			
10.	<b>Affiliation of authors</b>	NRSC, ISRO			
11.	<b>Originating unit</b>	GPDD/G&SPG / NRSC			
12.	<b>Sponsor(s)</b> <b>Name, Type:</b>	NRSC, ISRO, Govt. of India			
13.	<b>Date of Project Initiation</b>	April 2, 2014			
14.	<b>Date of Publication</b>	November 14, 2014			
15.	<b>Abstract:</b> This report describes a fully automated software algorithm development to realize snow albedo products from AWIFS data. The products were generated after doing a topographic correction to overcome the problems of differential illumination in rugged terrains like that of Himalayas. The narrow to broadband conversion coefficients which required for the estimation of albedos were simulated using 6S RT code. Comparison of the snow albedo estimated by the proposed method with the Landsat ETM snow albedo products, showed good correlation in different stages of snow metamorphism with $R^2$ value greater than 90%.				

---

# GENERATION OF BROADBAND SNOW ALBEDO PRODUCTS FROM AWIFS DATA

---

## 1. Introduction

Broad band Snow albedo is an important geophysical parameter for studies related to weather, climate, and hydrometeorology and so on. Snow has the highest albedo in nature and hence has a significant influence on surface energy budget and on Earth's radiative balance. It also serves as a key input to local or basin scale snow melt runoff models. The high sensitivity of snow to change in temperature and precipitation makes it a primary indicator of climate change. The albedo of snow is defined as the ratio of reflected to incident solar energy and is a function of sun angle, atmospheric parameters and cloudiness, and the size, shape, density and impurity contaminations of the snow crystals. Freshly fallen snow has a very high reflectance in the visible wavelength. As it ages, the reflectivity of snow decreases in the visible and especially in the longer (near-infrared) wavelengths. This can be due to the impurities that can get deposited over time or melting and refreezing process within the snow which lead to increased grain size [1]. The above said process leads to reduced reflectance from snow and hence a decrease in snow albedo. Remote sensing from satellite images provides an excellent method to observe and monitor global snow-cover distribution and evolution. Snow-cover mapping is being carried out at global, regional and basin wise scales using different satellite sensors. Various techniques, ranging from visual interpretation, multispectral image classification, decision trees, change detection and ratios have been used to map snow cover with multi spectral image data. The direct impact of snow cover, known as the snow albedo effect, can dramatically change the land surface energy budget and then influences air temperature, density, pressure, etc.

The Himalayan cryosphere has its importance because the presence of vast snow covers in the Himalaya due to its high elevations; also it is the source of water for some of the largest river basins of our country. The Himalayan Mountains have also been called the third pole, since they are the third largest body of snow on our planet after the Antarctic and Arctic. Large areas of the Himalaya are covered by seasonal snowfall during winter which starts ablating with the onset of spring, therefore, the areal extent of snow cover changes significantly from month of November to June [2] which greatly influences the land surface albedos and contributes an important feedback mechanism to global climate system.

Satellite imagery in mountainous terrain is affected due to sharp variations in the topographic parameters such as altitude, slope and aspect. The topographic variability causes a problem of differential illumination due to steep and varying slopes as in rugged

Himalayan terrain. Sun-facing illuminated slopes (south aspect) show more than expected spectral radiance or reflectance, whereas the effect is opposite in shadowed regions (north aspect). Therefore, a topographic correction which compensates the problem of differential solar illumination is essential for qualitative and quantitative analysis of snow cover applications.

For over three decades, satellites have been actively used for large-scale monitoring of snow cover from regional to global scales. Owing to frequent scene revisits, wide area coverage and high spatial resolution of RS2 AWiFS sensor, it can effectively supplement ground-based measurements and provide near real time spatially detailed information on the snow cover distribution. This document describes the AWiFS Broadband Snow Albedo Products for the Hindu Kush-Himalayan (HKH) regions covered by AWiFS acquisitions onboard Resourcesat-2. Broadband snow albedo is computed for solar wavelength region from 0.3 - 3.0 $\mu$ m. The snow bound regions in the AWiFS imagery were delineated using an automatic extraction algorithm based on the spectral reflectance pattern of snow in the various spectral bands of the sensor. AWiFS images were also subjected to topographic corrections. The topographic corrections are realized using slope matching techniques [3] which is reported to be most suitable for Himalayan terrain. These products are planned operational products to be delivered at 250m resolution.

## 2. Data Used

RESOURCESAT-2 was envisaged as a follow on mission to RESOURCESAT-1 data users with enhanced capabilities. Resourcesat-2 has a three-tier imaging capability, with a unique combination of payloads consisting of three solid-state cameras, viz., a high resolution Linear Imaging Self Scanning Sensor - LISS-IV, and two medium resolution cameras namely Linear Imaging Self Scanning Sensor - LISS-III and an Advanced Wide Field Sensor (AWiFS). AWiFS Sensor operates in four spectral bands providing a spatial resolution of 56 m and covering a swath of 740 Km. To cover this wide swath, the AWiFS camera is split into two separate electrooptic modules, AWiFS-A and AWiFS-B. The sensor characteristics are given in Table 1.

**Table 1. AWiFS Spectral Bands Characteristics**

Spectral Bands	Spectral Wavelength (nm)	Saturation radiance (mW/cm <sup>2</sup> /sr/ $\mu$ m)
B2	520-590	52.34
B3	620-680	40.75
B4	770-860	28.425
B5	1550-1700	4.645

RS2-AWIFS sub-scenes covering entire India was orthorectified using ETM ortho images which were subsequently used as master reference image for orthorectification. The product accuracy of rectified scenes is better than 1 pixel.

To address the effect terrain, we have used Advanced Spaceborne Thermal Emission and Reflection Radiometer (ASTER) Global Digital Elevation Model (GDEM). The ASTER GDEM covers land surfaces between 83°N and 83°S and is available in GeoTIFF format with geographic lat/long coordinates and 1 arc-second (30 m) grid of elevation postings. The vertical error of the DEM is reported to be less than 20 m. These data are currently distributed free of charge by the United States Geo-logical Survey (USGS) and are available for download from the site <http://earthexplorer.usgs.gov/>. The DEM was resampled to 56 m resolution to match the AWIFS sensor data and reprojected into an Albers equal-area projection. From the DEM, other topographic parameters, namely, slope, aspect and local illumination image have been derived for terrain correction using slope matching method.

### 3. Methodology

AWiFS Level-2 geo-referenced product along with meta file and AsterDEM is used for generation of snow albedo products. The flow chart depicting the methodology of processing steps involved in the estimation of the broad band snow albedo is given in Fig. 1. The algorithm for the generation of snow albedo is implemented in java with user friendly utilities like dynamic visualization, enhancement and progress status of input, output and intermediate files. The software is designed to support singlestrip/multistrip/tiled GeoTiff Ortho input files. Software operates in Single File / Batch Mode to handle single or multiple products respectively. The software is expecting precession corrected images, which is carried out manually.

In the following sections some the major processing steps are discussed in brief.

#### 3.1. Topographic Correction

Topographic correction was realized using slope matching technique which is well proven for the rugged terrains like that of Himalayas. The model is wavelength dependent which considers the mean illumination value to enhance the illumination of north facing slopes (or shady slopes) and equalizing their radiance with respect to sun facing slope. The topographically corrected spectral reflectance is estimates using eqn.

$$R_{n\lambda ij} = \left[ R_{\lambda ij} + (R_{max} - R_{min}) * \frac{(\langle \cos i \rangle_s - \cos i_{ij})}{\langle \cos i \rangle_s} \right] C_{\lambda} \quad (1)$$

Where  $R_{n\lambda ij}$  is normalized topographically corrected reflectance  $R_{\lambda ij}$  is reflectance on the tilted surface,  $R_{\max}$  and  $R_{\min}$  are max and min reflectance of the image,  $\langle \cos i \rangle_s$  is the mean illumination of sunny slopes  $\cos_{ij}(i)$  is illumination for pixel  $(i, j)$  and  $C_\lambda$  is normalization coefficient for different satellite bands and is estimated using equation (2)

$$C_\lambda = \frac{S'_\lambda - N_\lambda}{N'_\lambda - N_\lambda} \quad (2)$$

Where  $S'$  is the mean reflectance value on sunny slopes after first stage normalization,  $N$  is the mean reflectance value on shady slopes in uncorrected image,  $N'$  is the mean reflectance value on shady slopes after first stage normalization.

### 3.2. Snow cover extraction

The automated snow cover extraction is mainly based on Normalized Difference Snow index NDSI [4] values. The NDSI is a spectral band ratio that takes advantage of the spectral differences of snow in short-wave infrared and visible bands of AWIFS sensor. As snow has high reflectance in visible and very low reflectance in SWIR bands NDSI serve as an effective way to distinguish snow from other features in a scene. NDSI for AWIFS sensor is calculated as

$$NDSI = \frac{B2 - B5}{B2 + B5} \quad (3)$$

For pixels with NDSI value  $> 0.4$  it can be considered as candidate pixels for snow. Cloud is the only feature which has high reflectance value for visible bands as for snow and hence is often misclassified with cloud. To reduce the effect of snow/cloud misclassification we have used Normalized difference cloud index NDCI [5] proposed by Li et.al.

$$NDCI = \frac{B3 - B5}{B3 + B5} \quad (4)$$

NDCI value along with band5 reflectance is used to discriminate cloudy pixel from snow bound ones. NDCI value greater than 0.42 and band5 reflectance less than 0.11 together was used distinguish snow from cloud. In areas covered with snow and vegetation (mountain forests), the reflectance characteristic differs from both those of snow and vegetation spectra, since the reflectance characteristics are mixed together. It was observed that NDSI thresholding alone fails for detecting snow in mountain forests. For snow under vegetation, we used normalized snow index S3 [6].

$$S3 = \frac{B4(B3 - B5)}{(B4 + B3)(B4 + B5)} \quad (5)$$

S3 index uses the reflectance characteristics of both snow and vegetation in order to reduce errors caused by the mixed pixels containing both snow and vegetation, and to identify the snow-covered areas more accurately. Thresholding by S3 was done using dynamically arrived values using maximum value S3 for that particular scene. Apart from these normalized spectral indices, spectral band ratios of B3 & B4, B4 & B5, sum of reflectances of all bands (brightness) and also individual band reflectances are used to for the automated extracted of snow bound regions from AWiFS imagery.

Water and grey Cloud are the major noise features in the delineation of snow covered pixels. To discriminate water pixels from snow we have used normalized B4-B5 difference and B3/B4 ratio with suitable thresholding along with NDSI values and NIR reflectance as suggested by [7]. Grey clouds were also differentiated from snow using B2 and B5 reflectance values.

Thresholds were arrived by combining both visual interpretations and also by using statistical methods in more than 50 scenes acquired over different locations and at different periods of time. The thresholding conditions were implemented in a logical manner to delineate different kinds of snow from other features.

### **3.3. Narrowband to Broadband Albedo Conversion**

The Broadband (BB) surface albedo is determined for the entire short-wave range (0.3-3 $\mu$ m), satellite sensors provide only filtered albedo for some narrow spectral regions. If a surface is assumed to be Lambertian (the assumption most suitable to features like snow which have very little specular reflection), the retrieved surface reflectance of different spectral bands is equivalent to surface spectral albedo. The broadband surface albedo is calculated from narrowband satellite data by integrating band reflectance across the short wave spectrum [8] as given in eq (6)

$$\alpha = \sum_{b=2}^5 [\rho_b * w_b] \quad \text{----- (6)}$$

Where  $\rho_b$  is the surface reflectance of band b (b=2, 3, 4, 5 for AWIFS sensor) and  $w_b$  is the weighting coefficient representing the fraction of at surface solar radiation occurring within the spectral range represented by a specific band.

The weighting coefficients were computed with the inclusion of all wavelength regions that occurs between sensor bands. Broad band albedo was computed for the region 0.3- 3  $\mu$ m. The regions between satellite bands were arbitrarily divided between band edges. Figure 2 shows the reflectance spectra of medium grain snow taken from JHU library.

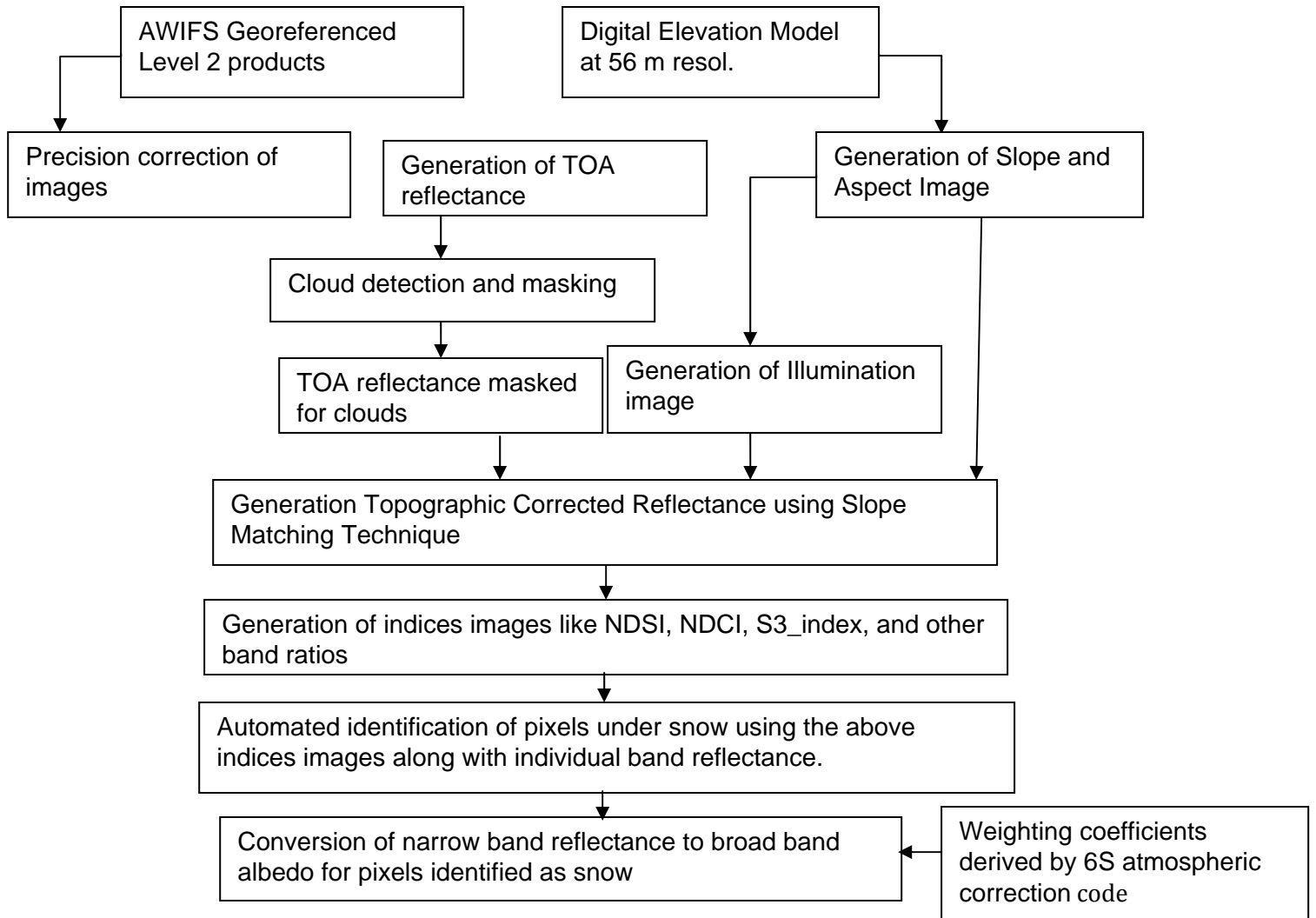


Fig. 1 Flow Chart showing processing steps involved in arriving at snow albedo products

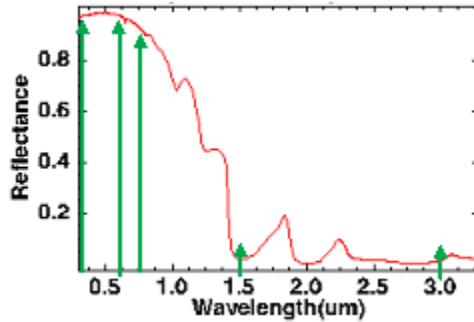


Figure 2. Spectral reflectance curve of snow (Source: John Hopkins University Spectral Library @ENVI)

The upper and the lower wavelength bound were fixed taking into consideration the reflectance spectra of snow as shown in Table2 below.

Table2. AWIFS Band Widths, Ranges for lower and upper wavelength bounds

Band	AWiFS Band limit( $\mu\text{m}$ )	Applied LW-UW bounds BB ( $\mu\text{m}$ )
2	0.52-0.59	0.3-0.6
3	0.62-0.68	0.6-0.75
4	0.77-0.86	0.75-1.5
5	1.55-1.70	1.5-3.0

The weights for the conversion of spectral albedo to broad band and visible albedo were computed using 6S atmospheric correction code [9]. The simulations were carried out with mid latitude winter atmospheric profiles for different combinations of Sun view angles, AOD, water vapor, ozone values. Final coefficients were arrived from these simulation results using averaging approach.

## 4. Results and Validation

Visual analysis of topographic corrected image using slope matching method with uncorrected image shows the reflectance value for all the bands have increased for the pixels falling in the north aspects. Figure 3 below compares AWIFS images before after correction. Visual validation was carried for different terrains and for different seasons.

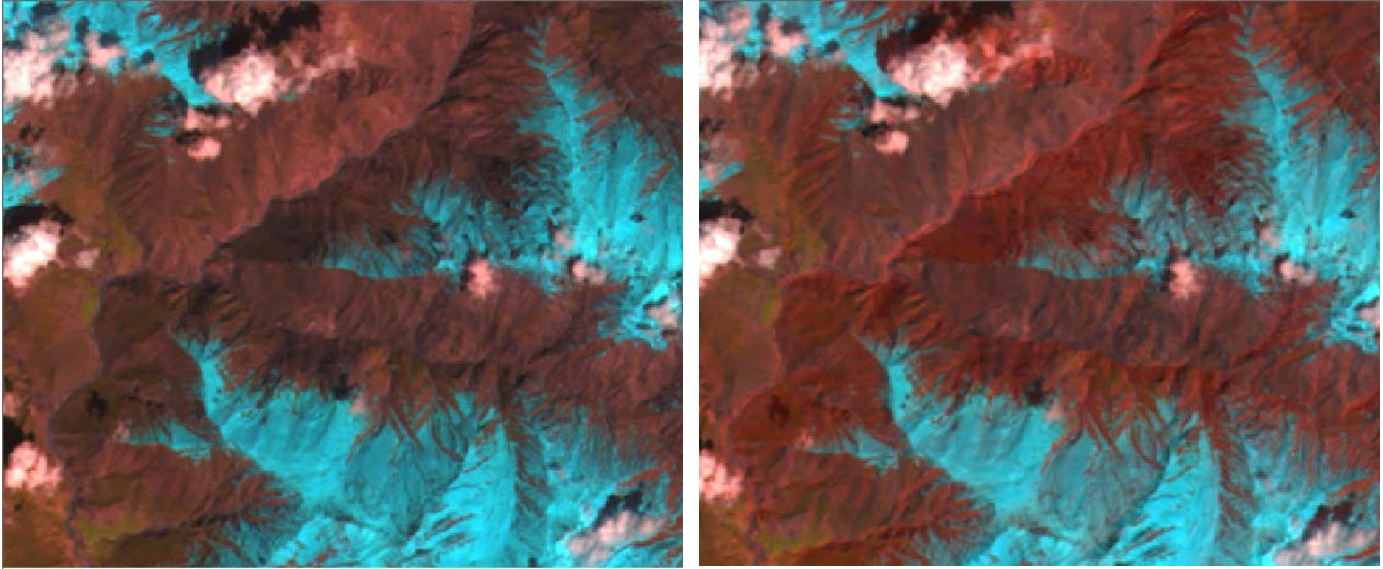


Fig.3(a) 96-48-b-24Apr2013 Before topographic Correction    96-48-b-24Apr2013 After topographic correction

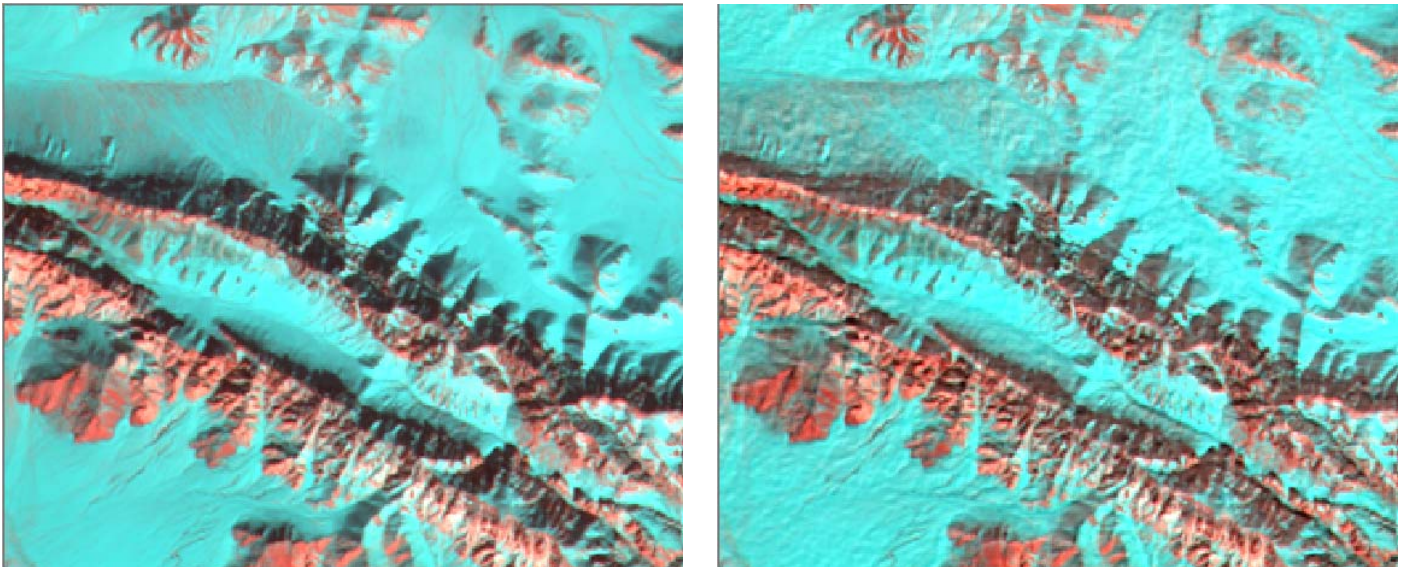


Fig. 3(b).97-48-b-23jan2013 Before topographic Correction    97-48-b-23jan2013 After topographic Correction

The results of the snow cover extraction were also validated visually using the corresponding input image. Snow albedo was then derived from these reflectance images by performing spectral correction of the narrow band reflectances to broadband albedo. Figure (4) shows snow albedo products in pseudo color along with the original FCC image and the snow cover extracted images for Jan and apr 2013. Figure (5) shows the snow albedo image along with the color bar depicting the range of values used in the images.

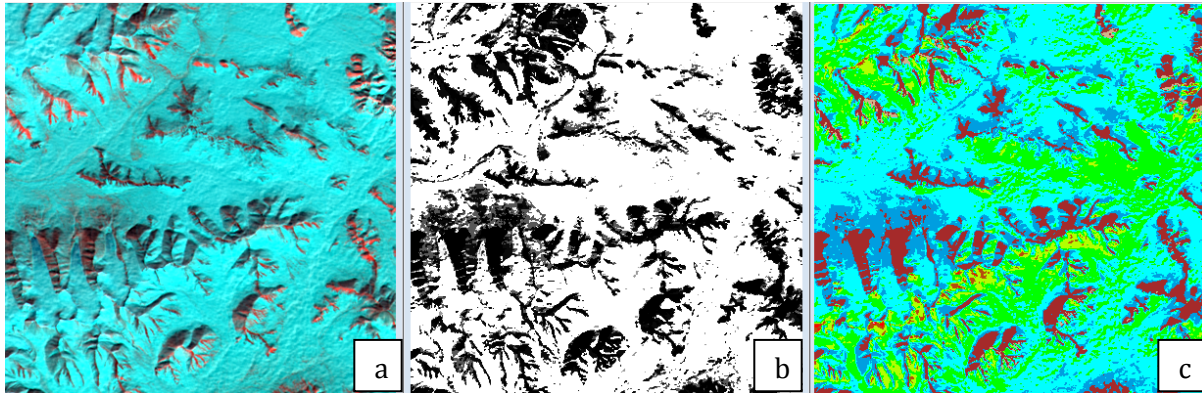


Fig. 4(i) 97-48-b-23jan2013 (a) Original FCC image (b) snow cover extracted image (c) Snow albedo image

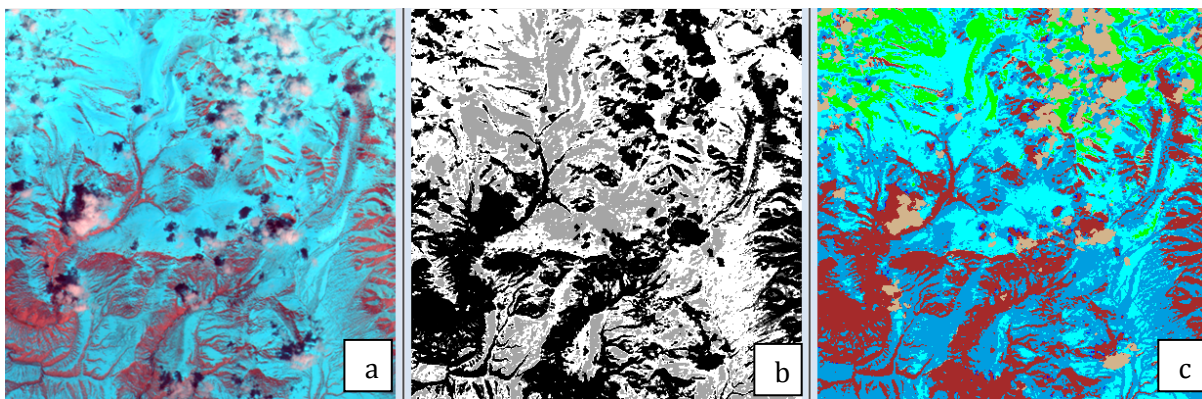


Fig. 4(ii) 96-48-b-24apr2013 (a) Original FCC image (b) snow cover extracted image (c) Snow albedo image

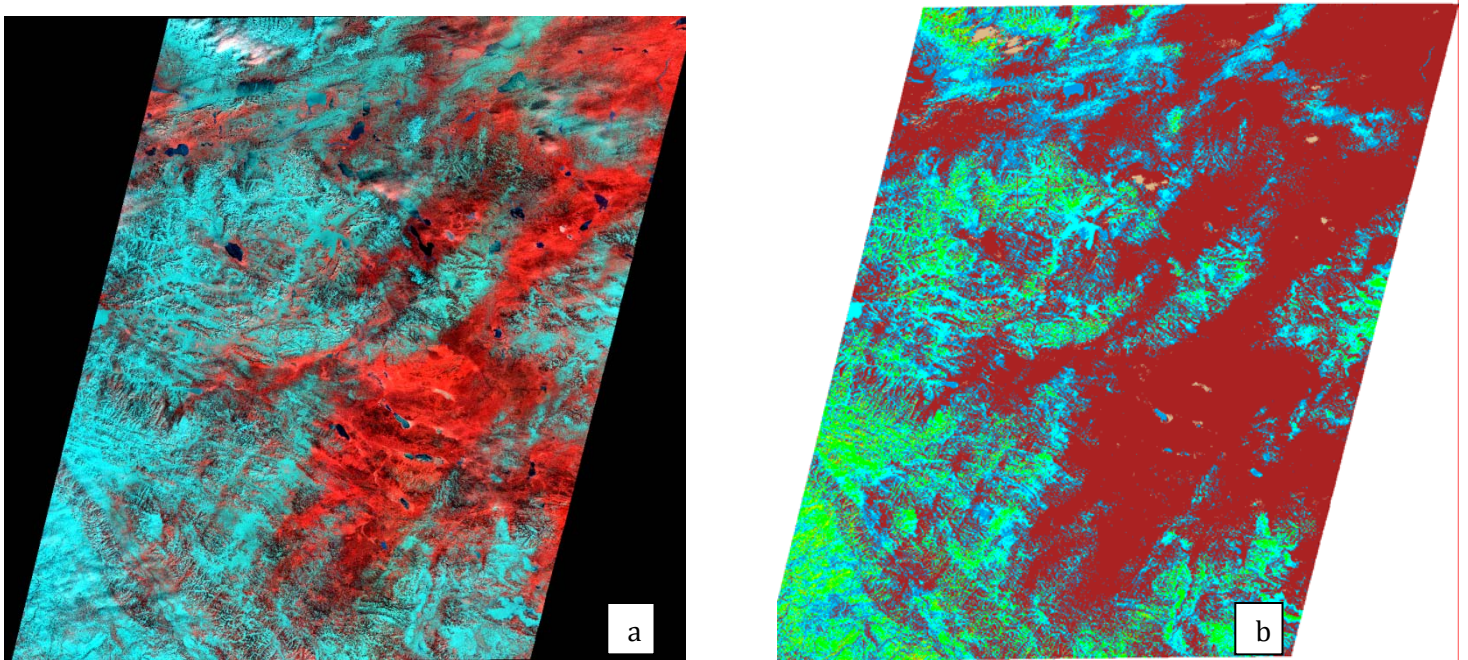
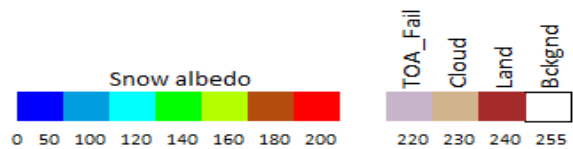


Fig. 5. 97-48-b-23jan2013 (a) Original FCC image (b) Snow albedo image with color ramp



The figure 6 below depicts the results of snow cloud discrimination. The clouds are depicted in tan color and land portions are given brown color.

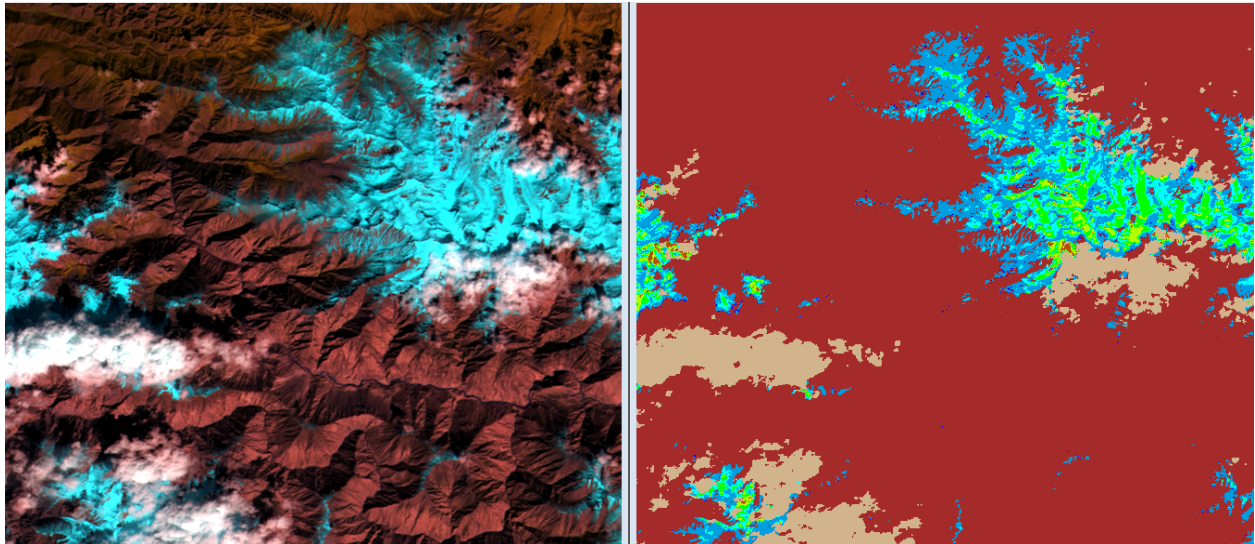


Fig. 6a. 96-43-d-10sep2014(a) Original FCC image

(b) Snow albedo image with color ramp

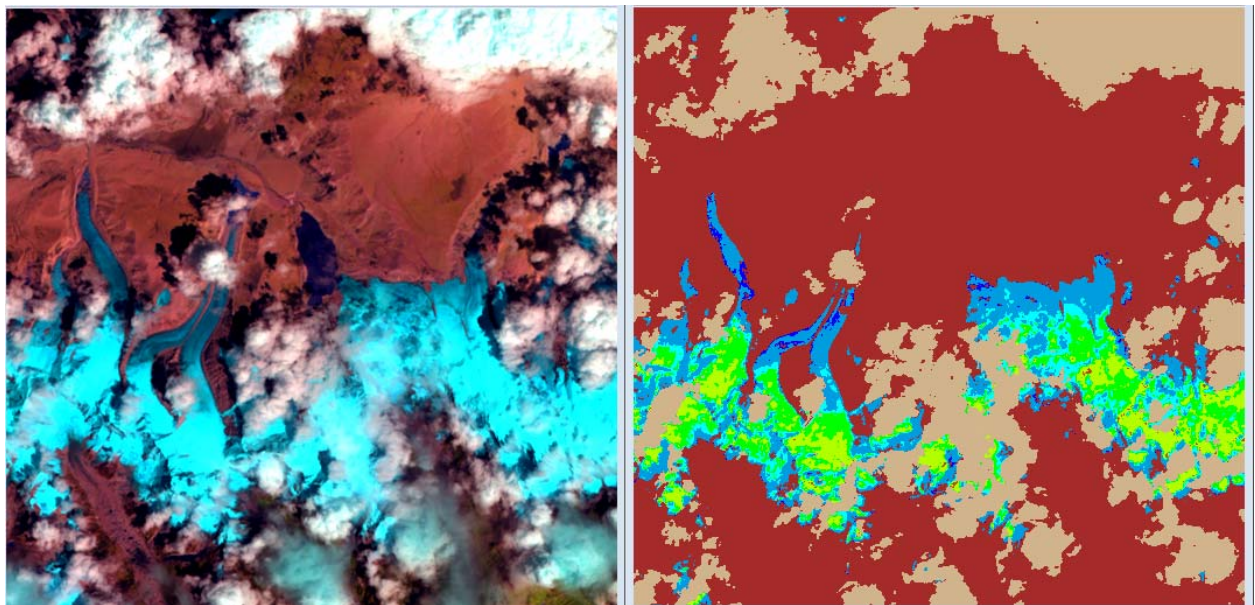
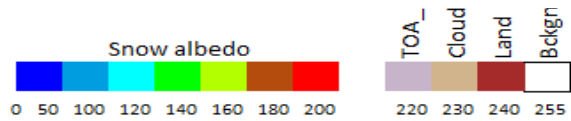


Fig. 6b 106-51-d-12sep2014(a) Original FCC image

(b) Snow albedo image with color ramp

The Snow albedo products realized using AWIFS Level2 data were validated using Landsat7 ETM+ snow albedo products. Though MODIS snow albedos are free downloadable because of the scale problems in comparing AWIFS products with MODIS, the validations were carried out using Landsat images. Landsat7 surface reflectance products are freely downloadable from the site [http://landsat.usgs.gov/CDR\\_ECV.php/](http://landsat.usgs.gov/CDR_ECV.php/). Broadband Snow albedo were then derived from surface reflectance of and band2(0.52 - 0.60) and band4(0.76 - 0.90) using the second order polynomial formula derived by Knap et al. [10] based on ground measurements of both glacier ice and snow.

$$\alpha_{short} = \frac{0.726\rho_2 - 0.322\rho_4^2 - 0.051\rho_4 + 0.581\rho_4^2}{0.726 + 0.581 - 0.322 - 0.0514}$$

Validation were carried for three months, namely Jan, Apr and Oct using sample point extracted from a set of three to four images per month. Seasonal analyses were carried to confirm the validity of the albedo products in different stages of snow metamorphism. The results of the validation are given in Figure 6. More than 90% correlation was observed between AWIFS and Landsat snow albedo products for each season.

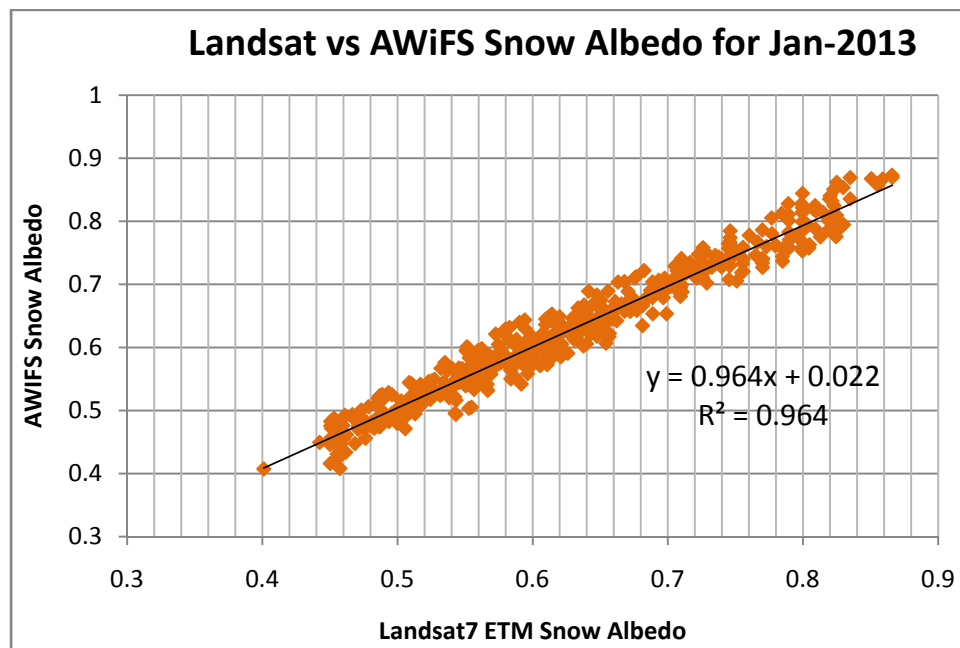


Fig. 7(a). Landsat7 Snow albedo and AWIFS Snow albedo Comparison for the month of Jan-2013

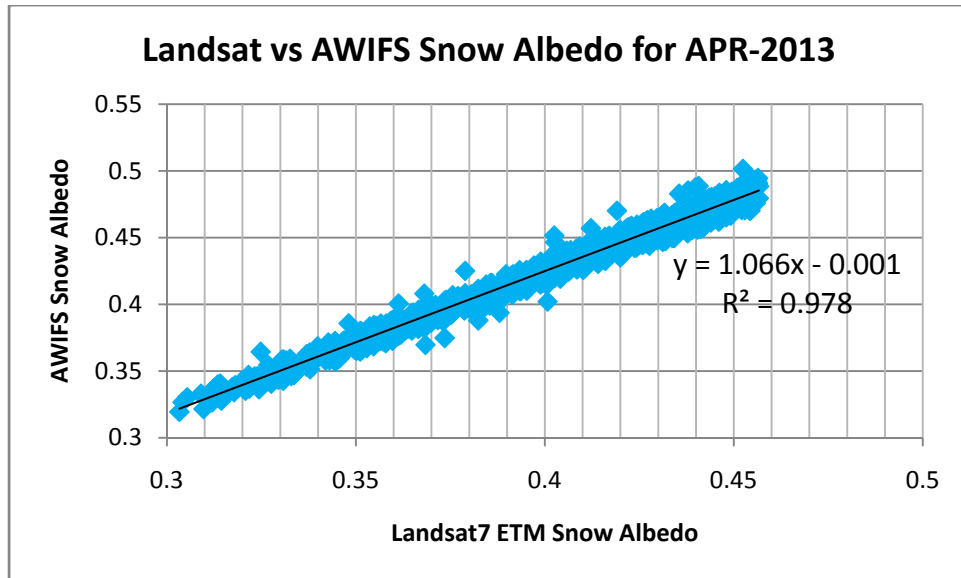


Fig. 7(b). Landsat7 Snow albedo and AWIFS Snow albedo Comparison for the month of Apr-2013

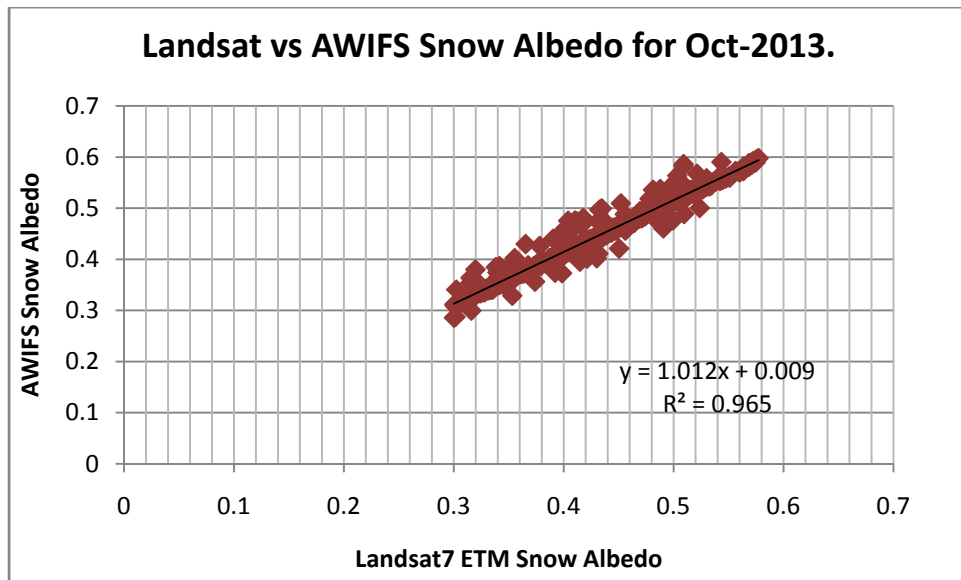


Fig. 7(c). Landsat7 Snow albedo and AWIFS Snow albedo Comparison for the month of Oct-2013

## Albedo products from AWIFS in BHUVAN

The snow albedo products from the above procedure are planned to be available in BHUVAN webportal shortly. The start and end date dates of each cycle are fixed for any month as 1-5, 8-12, 16-20 and 23-27. The products are delivered as quadrant scenes at 250m resolution.

### Products Formats Specification

• Image File Format	:	Geo TIFF
• Projection	:	Geographic Lat/Long
• Datum	:	WGS-84
• Spatial Resolution	:	250m
• Radiometric resolution (output)	:	8 bits per pixel
• Correction Level	:	precision corrected
• Number of bands	:	1
• DN – BB Albedo conversion rule	:	BB Albedo = DN/200 (in float)
• Usable range of DN	:	0 – 255
• Cloud	:	230
• Pixels other than cloud and snow	:	240
• Pixels with TOA values exceeds 1	:	220
• Image background	:	255

### File Naming Convention

Image file naming convention contains the following information:

- Satellite name
- Sensor name
- Product name
- Path and row
- Subscene
- Date of Pass
- Cycle number
- Version number
- Sub version number

Example: `irs_r2_awif_snowalbedo_100_92_A_18sep2014_cycle3_v01_01_byte.tif`

Figures 8 (a) and (b) below shows an image mosaic of quadrant scenes processed for second cycle of September and first cycle of October'14 respectively

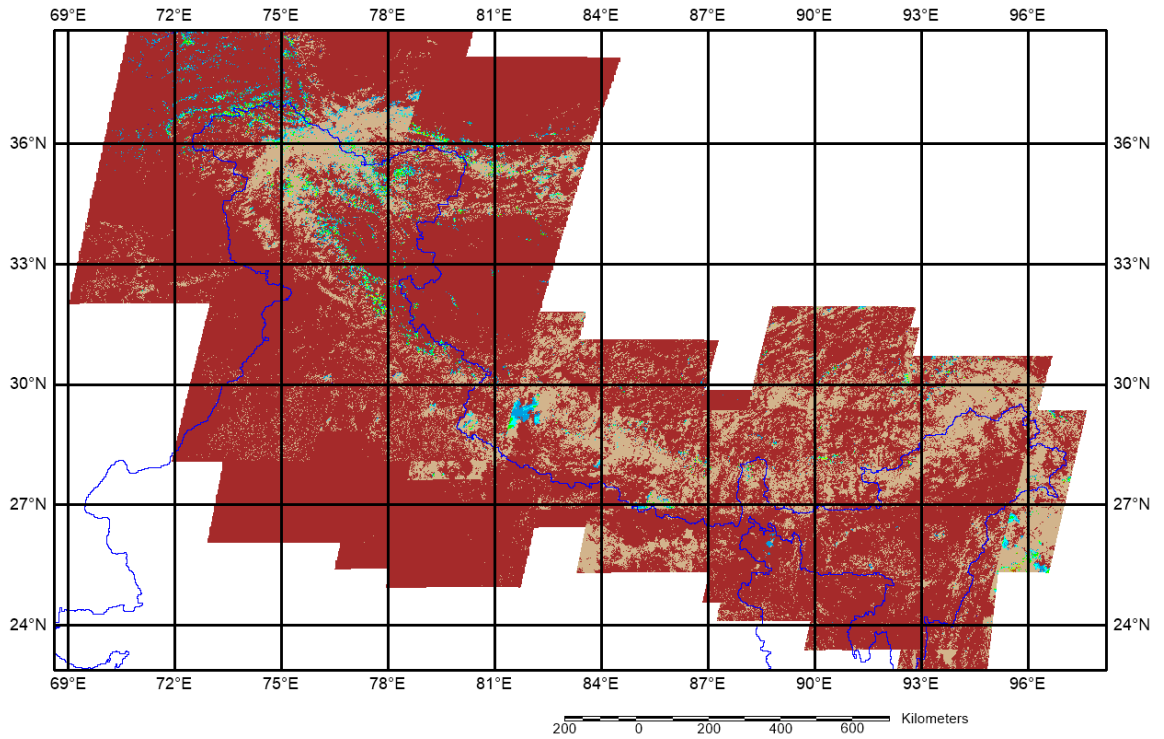


Fig 8(a) Snow Albedo mosaic for Cycle2 of Sep'14

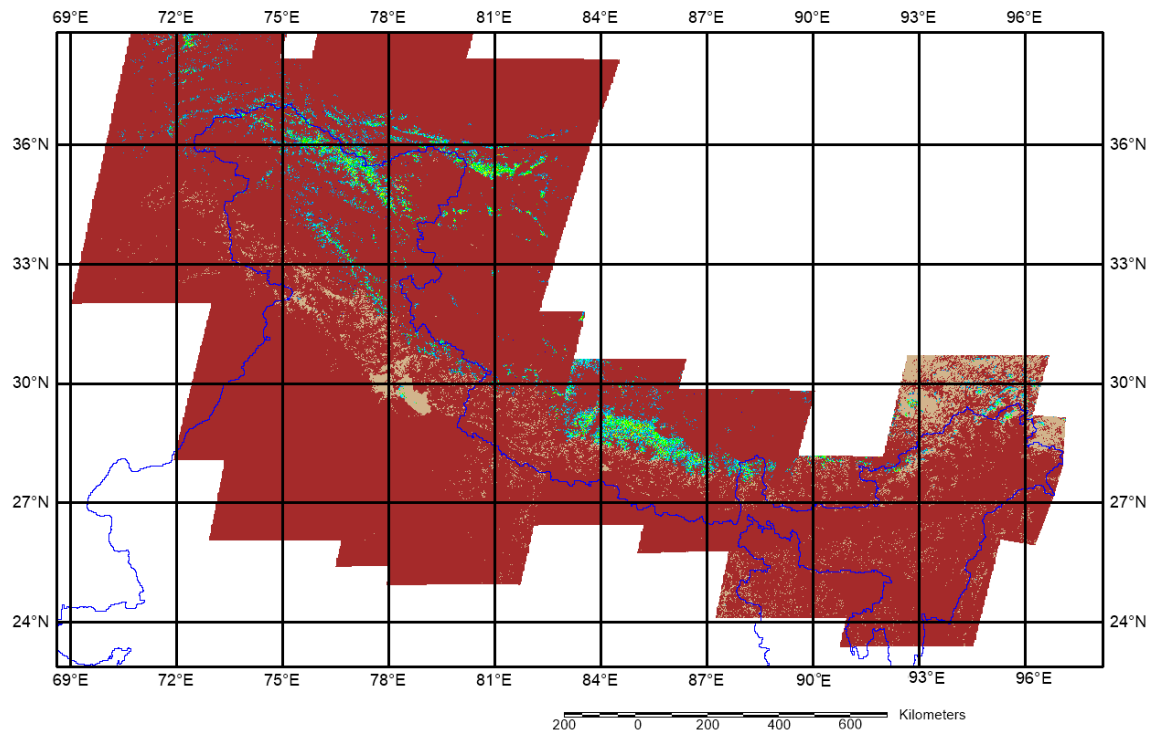


Fig 8(b) Snow Albedo mosaic for Cycle1 of Oct'14

---

## References

1. Dietz, A.J., Kuenzer, C., Gessner, U., and Dech, S. (2012). “Remote sensing of snow – a review of available methods”. *International Journal of Remote Sensing*, **33**, 4094–4134.
2. Mishra V D., Gusain, H. S. and Arora M K. (2012) “Algorithm to Derive Narrow Band to Broad band Albedo for snow using AWiFS and MODIS Imagery for Western Himalaya – Validation”. *International Journal of Remote Sensing Applications*, **2** (3) pp. 52-56.
3. Mishra V.D., Sharma, J. K., Singh., K K., Thakur N K and Kumar, M. (2009). “Assessment of different topographic corrections in AWiFS satellite imagery of Himalaya terrain”. *Journal Earth System Science*, Vol.**118** (1), pp.11-26.
4. Hall, D. K., Riggs, G. A., Salomonson, V.V. (2002). “Development of methods for mapping global snow cover using Moderate Resolution Imaging Spectrometer (MODIS) data”. *Remote Sensing of Environment*, **54**, 127-140.
5. Li, W., Fang, S., Dian, Y., and Guo, J. (2005). “Cloud detection in MODIS data based on spectrum analysis”. *Geomatics and Information Science of Wuhan University*, **30** (5), 435-438.
6. Shimamura, Y., Izumi, T., and Matsuyama, H. (2006). “Evaluation of a useful method to identify snow-covered areas under vegetation – comparisons among a newly proposed snow index, normalized difference snow index, and visible reflectance”. *International Journal of Remote Sensing*, **27** (21), 4867–4884.
7. Subramaniam, S., Suresh Babu, A.V., Sivasankar, E., Rao, V.V., and Behera, G. (2011). “Snow Cover Estimation from Resourcesat-1 AWiFS – Image Processing with an Automated Approach”. *International Journal of Image Processing*, **5** (3), 298-320.
8. Masahiro Tasumi; Richard G. Allen; and Ricardo Trezza(2008). “At-Surface Reflectance and Albedo from Satellite for Operational Calculation of Land Surface Energy Balance”. *Journal Of Hydrologic Engineering* , pp.51-63
9. Zhao, W., Masayuki Tamura, M., and Takahashi, H. (2001). “Atmospheric and Spectral Correction for estimating surface albedo from satellite data using 6S code.” *Remote Sensing of Environment*, **76** (2), 202-212.
10. W. H. Knap, C. H. Reijmer & J. Oerlemans. (1999). “Narrowband to broadband conversion of Landsat TM glacier albedos”. *International Journal of Remote Sensing*, **20** (10), 2091-2110.